



Thermodynamic studies of adsorption of rhodamine B and Congo red on graphene oxide

Juma Sahar^{a,*}, Abdul Naeem^a, Muhammad Farooq^a, Shah Zareen^a, Ata urRahman^b

^aNational Centre of Excellence in Physical Chemistry, University of Peshawar, Peshawar, 25120, Khyber Pakhtunkhwa, Pakistan, email: jsahar14@yahoo.com (J. Sahar)

^bInstitute of Chemical Sciences, University of Peshawar, Peshawar, 25120, Khyber Pakhtunkhwa, Pakistan

Received 22 January 2019; Accepted 19 May 2019

ABSTRACT

In the present work, graphene oxide was prepared by the modified Hummer's method for the effective removal of rhodamine B and Congo red from their aqueous solution. The synthesized graphene oxide was characterized by different techniques such as thermogravimetric/differential thermal analysis, scanning electron microscopy, Fourier transform infrared spectrometry and X-ray diffraction. It was found that among different models applied, the Langmuir isotherm model fitted the data very well for both the rhodamine B and Congo red dyes adsorption onto the graphene oxide. Moreover, Van't Hoff equation was used to calculate the various thermodynamic parameters such as, enthalpy (ΔH°), entropy (ΔS°) and Gibbs free energy (ΔG°) for both the selected dyes. The ΔH° for rhodamine B and Congo red was found to be 4.18 kJ mol⁻¹ and 10.69 kJ mol⁻¹ whereas, ΔS° was found to be 5.95 J mol⁻¹ K⁻¹ and 8.80 J mol⁻¹ K⁻¹ respectively. Similarly, the Gibbs free energy (ΔG°) was calculated to be -1.89 kJ mol⁻¹ and -2.78 kJ mol⁻¹ for rhodamine B and Congo red respectively. The thermodynamic studies indicated that the entire adsorption process was physisorption, endothermic and spontaneous in nature. The high adsorption affinity of the graphene oxide could be due to the electrostatic interaction between the positively charged surface of rhodamine B and negatively charged surface of graphene oxide. Further, this study depicts that the synthesized graphene oxide has a great potential to remove the dyes from waste water effectively.

Keywords: Graphene oxide; Rhodamine B; Congo Red; adsorption; Langmuir adsorption isotherm

1. Introduction

Water is an indispensable part of life as most of the human metabolic activities also depend upon water. Water is used for drinking, cleaning, bathing, air conditioning, washing and heating. Water containing pollutants affect the natural level of environment. Any undesirable change in the chemical, physical and biological properties of the water lead to harmful effects on the human life as well as the natural environment [1].

Approximately 3% of the entire earth surface water is fresh water. A very small proportion of this water is available for the human society [2]. The toxic effluents from industries and agriculture sector are significant threat to the

environment [1]. Similarly, domestic and municipal wastes are also responsible for water pollution. In the above context, fresh water in general and particularly in Pakistan is becoming unsafe for the use of human purposes [2].

Dyes are the main cause of water pollution and becoming the major environmental problem in the universe. Dyes have low biodegradability, affects human beings and natural ecosystem as well [3]. Different dyes are used for different purposes by textiles, dyeing operations, printing, food and paper making industries [4–6]. Colored effluents coming from the textile, paper, plastic, dyeing and printing industries containing Congo red and rhodamine B [5,7].

Congo red having anionic nature in solution belongs to diazo dye and it is the first synthetic dye used for dyeing cotton. Congo red dye upon metabolization produces benzidine which is known to be human carcinogen [8,9]. It also

*Corresponding author.

causes irritation to eyes, skin, gastro intestine and affects blood clotting as well as induces the respiratory problems. Congo red dye is optically, thermally and physiochemically stable [10,11]. Therefore, biodegradability of this dye is difficult due to its complex aromatic nature. This dye is also sensitive towards the pH and its color changes from red to blue as the pH of the solution decreases below pH 5 and becomes reddish in the pH range of 5–10 [8].

Similarly, Rhodamine B belongs to xanthene dyes and is soluble both in water and organic solvents. Due to its stability, it is used as a biological stain, pathology, histology and for dye laser production [12]. It can also be used for dyeing wool, jute leather, silk and cotton in textile industries. It is highly toxic and causes irritation to eyes, skin and respiratory tract if swallowed by humans and animals [13]. Due to the presence of N-ethyl groups on the sides of xanthene ring it is highly toxic and carcinogenic due to which it is banned in many countries while using for coloring of food and cosmetics [14].

Different physio-chemical techniques such as coagulation, ozonation, flocculation, chemical oxidation, ion exchange, reverse osmosis, photo catalysis, precipitation and adsorption are used for the treatment of different industrial waste effluents [15,16]. Among these techniques, adsorption process is the most effective technique which is successfully employed for the removal of color from wastewater [17]. Adsorption is more reliable process due to its simplicity, high efficiency, regenerability [15] and recycling of the adsorbent and low production of residues [16–18].

Different adsorbents like activated carbon, fly ash, manganese oxide, silica gel, soil, alumina, red mud, bentonite, kaolinite, hematite, biomass, polymers and clay [15,16] are used for the removal of toxins from aqueous system [19]. Yang et al. [20] studied the adsorptive removal of Congo red dye using functionalized carbon nanotube/mixed metal oxide and its maximum adsorption capacity was 1250 mg/g. Jia et al. [21] used 3D hierarchical porous iron oxides for the adsorptive removal of Congo red dye from waste water. The maximum adsorption capacity was obtained for α -Fe₂O₃. The removal performance was reported in the order of-Fe₂O₃ > Fe₃O₄ > γ -Fe₂O₃. Motahari et al. [22] studied the removal of rhodamine B from waste water using the NiO Nano particles in the presence of H₂ acacen ligand and the maximum monolayer capacity was observed to be 111 mg/g.

Graphene oxide displays excellent electronic, thermal, mechanical and optical properties. Therefore, it can be used in catalysis, electronics, sensors, and for energy conversion and storage [23]. Graphene oxide can also be modified by using nanomaterials, surfactants, biomolecules and polymers to enhance its efficiency for different applications. Graphene oxide has been used as an adsorbent for the adsorption of different dyes, aromatic wastes and heavy metal cations from water on account of its acidic nature and high surface area [24,25]. Graphene oxide can act as an excellent adsorbent for the removal of rhodamine B and Congo red. However, no systematic studies on the ion exchange removal of rhodamine B and Congo red from aqueous solutions by the graphene oxide have been reported in the literature. In the present work, graphene oxide has been utilized for the sorption of rhodamine B and Congo red from aqueous solutions. Moreover, the effect of

pH has also been evaluated in order to develop an efficient process for the removal of selected dyes under suitable conditions.

2. Experimental

2.1. Materials and chemicals

Graphite powder was purchased from Daejung chemicals, potassium permanganate, sulphuric acid, hydrochloric acid, sodium nitrate, sodium hydroxide and hydrogen peroxide, were purchased from Scharlau. Rhodamine B having a molecular weight equal to 479.01 g/mol and a molecular formula C₂₈H₃₁N₂O₃Cl was purchased from BioM laboratories Cerritos USA (Chemical Division, Malaysia) and Congo red dye having a molecular formula C₃₂H₂₂N₆Na₂O₆S₂ and molecular weight equal to 696.665 g/mol was obtained from BDH chemical Ltd Poole England. All the chemicals used during the whole studies were of analytical grade.

2.2. Graphene oxide syntheses

The graphene oxide was synthesized by using modified Hummer's method [26]. Typically, 3 g of graphite powder was dissolved in 70 mL of concentrated sulphuric acid (H₂SO₄) in the double walled cell and the temperature of the system was kept below 10°C. The mixture was stirred for 30 min and then 9 g of KMnO₄ was added slowly and the temperature was maintained lower than 5°C. The mixture was stirred and the temperature was allowed to increase gradually. When the temperature reached to 40°C, about 150 mL of deionized water (H₂O) was added slowly to the mixture and the temperature was raised up to 90°C. Then 500 mL of deionized water was further added which was followed by the addition of 15 mL of 30% H₂O₂. As a result, the color of the solution changed from dark brown to yellow and the suspension was stirred to make it homogeneous. The material was filtered and washed with 10% HCl solution to remove metal ions. The as synthesized material was again dispersed in 1000 mL of deionized water and kept overnight. The suspension was centrifuged and washed with deionized water until the pH became neutral. The obtained particles (graphite oxide) were dispersed in deionized water and sonicated to get the graphene oxide dispersion. The graphene oxide dispersion was then centrifuged and dried in oven at 100 for further studies [26,27].

2.3. Characterization of graphene oxide

Different analytical techniques such as thermogravimetric/differential thermal analysis (TG/DTA), scanning electron microscopy (SEM), fourier transform infrared spectrometry (FT-IR) and X-ray diffraction (XRD) were used for the characterization of the synthesized graphene oxide before and after adsorption studies.

2.4. Adsorption studies

Batch adsorption experiments were performed in order to obtain the rate and data of equilibrium. About 40 mL of each rhodamine B and Congo red (1.4 × 10⁻⁴ M) was taken into 100

mL titration flasks separately and then 0.1 g of adsorbent was added to each reaction vessel. The reaction mixtures were equilibrated for 24 h at 298 K in the shaker bath. The suspension was then filtered by using the Whatman filter paper 44 to separate the graphene oxide. The supernatant solution absorbance was then determined in order to calculate the concentration of residual dyes. UV-Visible spectrophotometer (BMS VIS-1100) was used to measure the concentration before and after the treatment of graphene oxide with selected dyes in the wavelength range of 498 to 554 nm. Initial concentration of dye and adsorbent dosage were varied to study their effect on the adsorption kinetics. In order to observe the pH effect on the dyes adsorption, the adsorption process was carried out in the pH range of 2–10. The solutions pH was adjusted by using HCl/NaOH solutions and pH meter. The studies of adsorption were performed at various temperatures, such as 298 K, 308 K and 318 K, in order to find the effect of temperature on the thermodynamic parameters. The sorption amount at time t , q_t (mg/g or mol/g) was calculated by using the following equation:

$$q_t = \frac{(C_o - C_t)V}{W} \quad (1)$$

where C_t (mg/L or mol/L) is the dye liquid phase concentration at any time, C_o (mg/L or mol/L) is the initial concentration of dye in the solution, V (L) is the solution volume and W (g) is the graphene oxide mass.

The equilibrium sorption capacity amount q_e (mg/g or mol/g) was determined by using the following equation:

$$q_e = \frac{(C_o - C_e)V}{W} \quad (2)$$

The percent removal of rhodamine B and Congo red can be determined from the following equation:

$$q_e = \frac{(C_o - C_e)}{C_o} \times 100 \quad (3)$$

where C_o and C_e (mg/L or mol/L) are the initials and an equilibrium liquid phase concentration of the rhodamine B and Congo red in the solution.

3. Results and discussion

3.1. Characterization of graphene oxide

3.1.1. X-ray diffraction analysis (XRD)

The X-ray diffraction (XRD) analysis was performed to achieve the information about the degree of oxidation. Fig. 1 shows the XRD pattern of the synthesized graphene oxide. It can be observed that only one peak appeared at the $2\theta = 10.5^\circ$ in the XRD pattern of the graphene oxide which corresponds to (001) plane. This confirms that the sample of graphene oxide was synthesized successfully. The present findings are in close agreements with the literature [28,29].

3.1.2. Thermal gravimetric analysis (TGA)

The thermogravimetric analysis was used to measure the weight loss in the graphene oxide as shown in Fig. 2. It

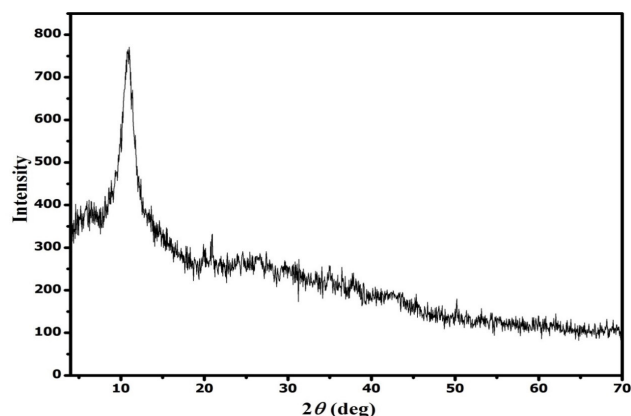


Fig. 1. XRD pattern for graphene oxide.

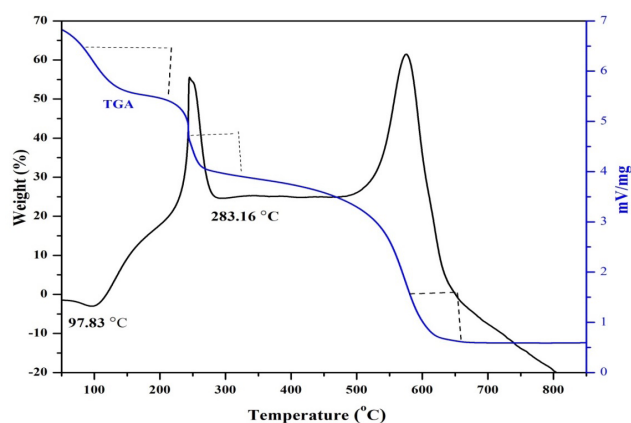


Fig. 2. TG/DTA of graphene oxide at 1273 K.

can be observed from the thermogravimetric curve that the graphene oxide is thermally unstable and starts to lose its weight upon heating. Further, it can be observed that the weight loss of graphene oxide was observed in three stages. In the first stage i.e. from 70–140°C the weight loss could be attributed to the removal of adsorbed water. A high weight loss could be observed at 200°C, which may be due to the removal of oxygen containing groups in graphene oxide in the form of CO_2 and H_2O . The peak appeared at 550°C is attributed to the weight loss due to the combustion of carbon skeleton of graphene oxide [30]. Similarly, the DTA curve also supported the three weight losses at about 97.83°C, 283.16°C and 600°C.

3.1.3. Scanning electron microscopy (SEM)

SEM is widely used for the surface and morphological characteristics of the adsorbent material. It also deals with the porosity and surface texture of the adsorbent and plays an important role in the surface availability determination for the dyes adsorption onto the adsorbent. Fig. 3a shows the SEM images of synthesized graphene oxide before adsorption while Figs. 3b and 3c show the SEM images of graphene oxide after the adsorption of rhodamine B and Congo red respectively. Before the adsorption, the graphene

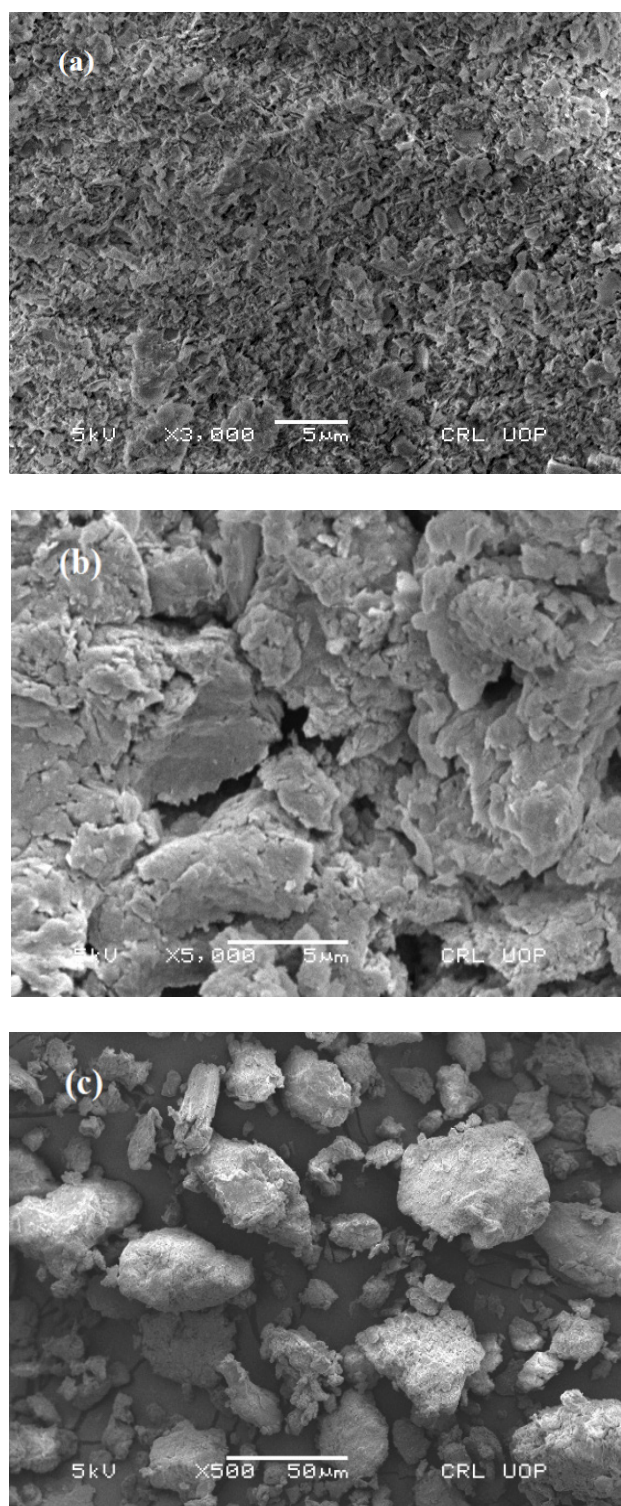


Fig. 3. SEM micrograph of graphene oxide (a) before adsorption and (b & c) after rhodamine B and Congo red adsorption respectively.

oxide particles are highly porous while after adsorption the surface of graphene oxide is loaded with rhodamine B and Congo red and the graphene oxide becomes bulky and the

particles are agglomerated and becomes spherical in shape [31,32].

3.1.4. Fourier transform infrared spectroscopy (FTIR)

FTIR was used to identify the functional groups that are responsible for the rhodamine B and Congo red adsorption onto the surface of graphene oxide. Fig. 4 shows the FTIR spectra of graphene oxide before and after the rhodamine B and Congo red adsorption. Different oxygen containing functional groups could be observed in the FTIR spectra. The main absorption band recorded at 3340 cm^{-1} could be assigned to the stretching vibrations of O-H groups. The peaks of absorption at 1730 and 1630 cm^{-1} could be due to the C=O stretching of carboxylic and carbonyl functional groups respectively. While the two peaks of absorption appeared at 1226 cm^{-1} and 1044 cm^{-1} are due to the stretching vibrations of C-O [31]. After the rhodamine B adsorption, strong characteristic band appeared at 821 and 1331 cm^{-1} (Fig. 4b). These absorption bands could be assigned to the adsorption of rhodamine B onto the graphene oxide surface [33]. Similarly, the absorption peaks at 1182 cm^{-1} (Fig. 4c) is associated with the benzene rings vibrations and the peak at 1045 cm^{-1} is assigned to the stretching vibration of S=O bond [34]. Thus, it is concluded from the FTIR analysis, that rhodamine B and Congo red dyes were successfully adsorbed onto the surface of graphene oxide.

3.1.5. Point of zero charge of graphene oxide

Point of zero charge (PZC) of the graphene oxide was determined by the salt addition method. 40 mL of NaNO_3 was taken in various conical flasks and then the pH of these solutions was adjusted in the range of 1 to 11 using NaOH/HCl . About 0.1 g of adsorbent (graphene oxide) was then added to each flask and kept for 24 h in a shaker bath. After 24 h , the pH of each suspension was determined and finally the pH versus pH_i was plotted to calculate the PZC for graphene oxide as shown in Fig. 5. The PZC for graphene oxide was calculated to be 2, which is in close agreement with the reported values [35–37]. At this pH, graphene oxide behaves neutrally. The surface is positively charged below the PZC and adsorption of anionic dyes is most favourable while the surface is negatively charged above the PZC which adsorbs preferably the cationic dyes. Graphene oxide consists of a several functional groups such as epoxy, hydroxyl, ketone and carboxyl groups. When graphene oxide is dispersed in water, a negative charge is created on its surface because of the ionization of the surface functional groups. The PZC graph demonstrates that the surface of graphene oxide remains negatively charged almost over the entire pH range (above pH_{PZC} value 2).

3.2. Adsorption studies

3.2.1. pH effect on adsorption of rhodamine B and Congo red

The pH plays an important role in the dyes adsorption onto the adsorbent surface. The surface charge of the adsorbent and the degree of ionization of the dye are dependent upon the change in the pH of the solution. The solution pH

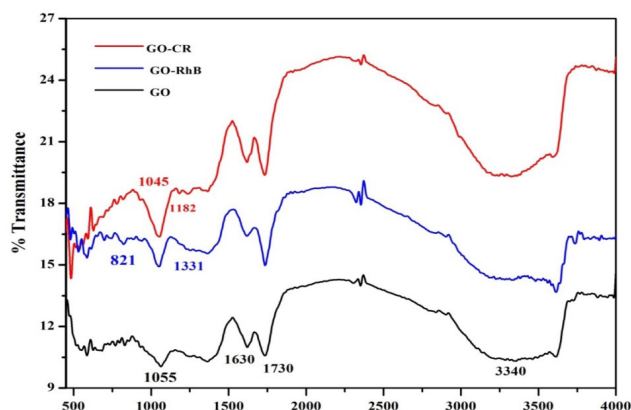


Fig. 4. FTIR spectra of graphene oxide (a) before and (b & c) after adsorption of rhodamine B and congo red respectively.

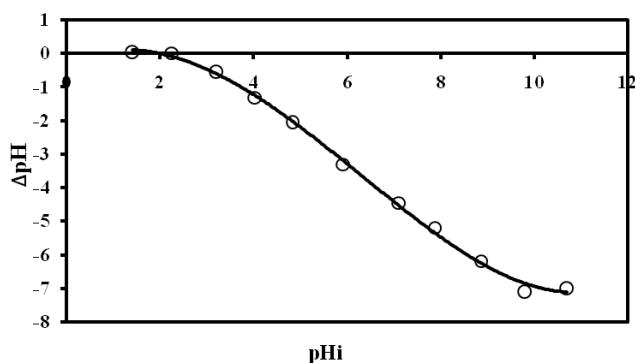


Fig. 5. Point of zero charge (PZC) of graphene oxide.

also changes the color intensity and structural stability of the dyes [38]. The adsorption data collected at various pH are given in Fig. 6a. It can be seen that the adsorption of rhodamine B increases with the increasing solution pH. The pH adsorption curve shows that the uptake of rhodamine B is strongly dependent on initial pH of the solution. Further, it can be observed that the rhodamine B removal from aqueous solution increases almost linearly with the increase in the pH. However, at pH 7 the curve was leveled off and no further change in the adsorption capacity of the graphene oxide was noted. This indicates the saturation of the graphene oxide surface. The decrease in the rhodamine B adsorption at pH 2 could be assigned to the electrostatic repulsion between the negatively charged surface and rhodamine B. While the increase in the uptake of rhodamine B in alkaline pH region can be attributed to the electrostatic attraction between the negatively charged surface and cationic dye [35,37]. While the effect of pH on Congo red dye adsorption is shown in Fig. 6b. As can be seen that the Congo red adsorption decreases with an increase in the solution pH. The pH adsorption curve shows that the uptake of Congo red is strongly dependent on initial solution pH. Graphene oxide contains several oxygen functional groups such as carboxylic (-COOH), epoxy and hydroxyl (-OH) groups. Therefore, when it is dispersed in aqueous solution it exist in anionic form due to carboxylic groups (-COOH) which are present in carboxylate (-COO⁻)

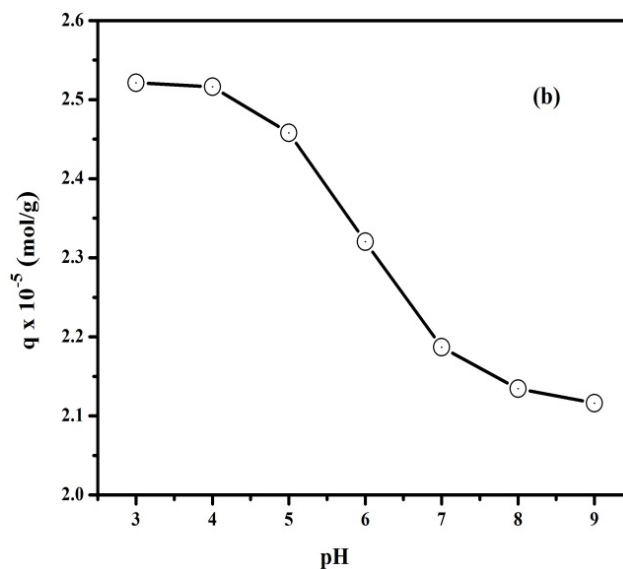
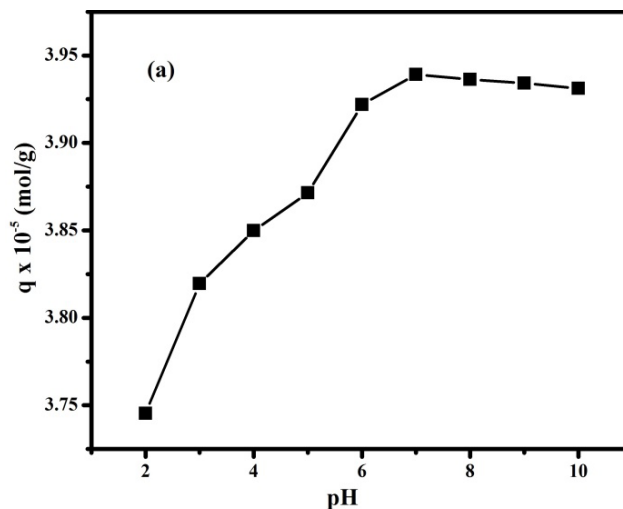


Fig. 6. pH Effect on dye (a) rhodamine B and (b) congo red removal onto graphene oxide at 298 K.

form. On the other hand, the Congo red dye is dipolar in nature. The Congo red dye may exist either as a cationic or anionic form depending on the pH of the solution. At lower pH, the NH₂ and -SO₃⁻ groups of the Congo red dye are protonated and converted to the NH₃⁺ and -SO₃H respectively and show attraction towards the negative surface of the graphene oxide which results in the maximum adsorption at pH 3 while at higher pH the Congo red exist as negatively charged -SO₃⁻ due to the deprotonation of the dye and showing repulsion towards the negatively charged graphene oxide surface [39,40]. As such, the adsorption of Congo red decreases with the increase in the pH of the solution. But due to its sensitivity towards the acids, the color of Congo red changes from red to blue with the change in solution pH i.e. at low pH and in the pH range of 5–10 it becomes reddish [11]. Consequently, pH 7 was chosen for further studies because at this pH the dye remains stable and no change in the color was observed at this pH value.

3.3. Adsorption isotherms

The adsorption isotherms are used to study the adsorption performance in the process of adsorption and define the interactions between adsorbent and adsorbate. In the present studies, various isotherms such as Langmuir, Freundlich and Dubinin-Radushkevich were used to interpret the experimental data.

3.3.1. Langmuir adsorption isotherm for rhodamine B and Congo red adsorption

The monolayer formation on the adsorbent surface is best defined by the Langmuir adsorption isotherm. According to this model, a uniform adsorption of adsorbate molecules on certain specific sites of the adsorbent takes place. Further, the adsorption sites are energetically uniform and there is no adsorbate transmigration on the plane of the adsorbent surface [41,42]. The linear form of the Langmuir adsorption isotherm, which is based on the above assumptions, can be represented as follow.

$$\frac{C_e}{q} = \frac{C_e}{q_m} + \frac{1}{K_L q_m} \quad (4)$$

where C_e (mg/L or mol/L) is the concentration of dye at equilibrium present in the solution, q is the amount of adsorbed dye per unit mass of adsorbent (mg/g or mol/g), q_m is the area occupied by the adsorbate monolayer, indicating the adsorption capacity (mg/g or mol/g), K_L is the Langmuir isotherm constant (L/mg) and associated to the adsorption free energy. The values of q_m and K_L for the rhodamine B and Congo red adsorption were obtained from the slope and intercept of the plot of C_e/q versus C_e as presented in the Fig. 7a-b. The theoretically calculated monolayer adsorption capacities from the Langmuir isotherm and experimental results for selected dyes are shown in Table 1 and 2. The experimental adsorption capacities are in close agreements with the theoretical adsorption capacities, which indicate that Langmuir model is best fitted to the experimental data of rhodamine B and Congo red adsorption onto the graphene oxide [43,44]. The monolayer adsorption capacity value slightly increases with increase in temperature from 298 to 318 K. The values of q_m and K_L concludes that maximum removal relates to the monolayer saturation of the molecules of adsorbate on surface of adsorbent with constant energy and no adsorbate transmission occurred in the plane of the surface of adsorbent. Further, the value of K_L shows that the entire process is endothermic in nature. The separation factor (R_L) was calculated (Tables 1 and 2) to confirm the favorable nature of the adsorption process. The Langmuir adsorption isotherm important characteristic can be expressed in term of dimensionless constant referred to equilibrium parameter or separation factor R_L and the shape of isotherm can be indicated from the value of R_L .

$$R_L = \frac{1}{(1 + K_L C_i)} \quad (5)$$

where C_i is adsorbate (dye) initial concentration present in the solution and K_L is the constant of Langmuir isotherm. The value of R_L shows the type of isotherm to be linear ($R_L = 1$), irreversible ($R_L = 0$), unfavorable ($R_L > 1$) and favorable (0

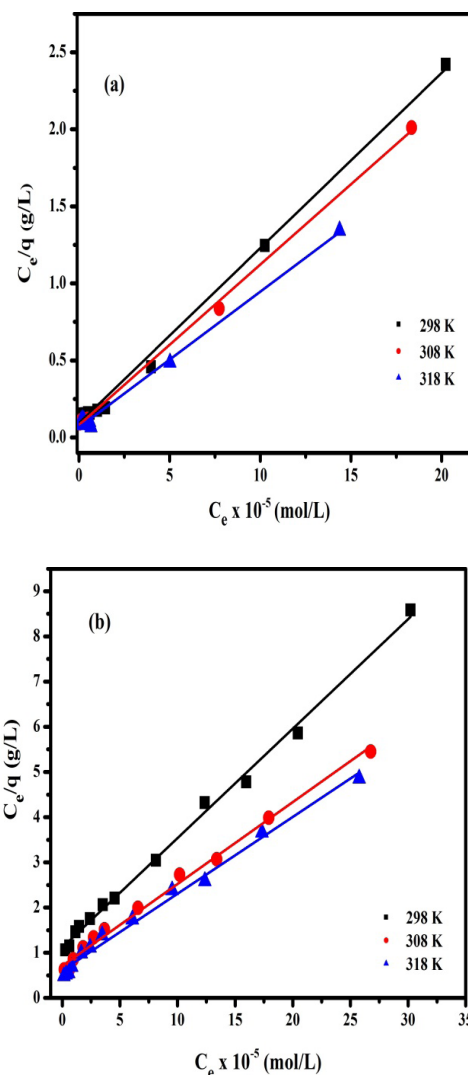


Fig. 7. Langmuir isotherm for the removal of dye (a) rhodamine B and (b) congo red onto the surface of graphene oxide at pH 7.

$< R_L < 1$). The calculated values of R_L at all initial concentrations of both rhodamine B and Congo red were found to be in the range of 0–0.01, which confirms that the rhodamine B dye uptake was favorable on graphene oxide [45].

3.3.2. Freundlich adsorption isotherm for rhodamine B and Congo red adsorption

Freundlich isotherm is used for the heterogeneous surfaces adsorption that involves the interaction between the molecules adsorbed. This model is not limited to the monolayer formation and the sorption energy decreases exponentially on the completion of the adsorbent sorption sites [46,47]. This isotherm is used for the determination of the adsorption intensity and capacity of the adsorbent. The empirical equation of the Freundlich isotherm is given below,

$$q_e = K_F \cdot C_e^{1/n} \quad (6)$$

Table 1
Langmuir parameters for the rhodamine B adsorption onto the surface of graphene oxide at different temperatures and pH 7

Temperature (K)	Theoretical $q_m \times 10^{-5}$ (mol g ⁻¹)	Experimental $q \times 10^{-5}$ (mol g ⁻¹)	R ²	K_L (g/L)
298	8.79	8.69	0.996	1.233
308	9.60	9.44	0.997	1.294
318	11.33	10.70	0.963	1.371

Table 2
Langmuir parameters for the congo red adsorption onto the surface of graphene oxide at different temperatures and pH 7

Temperature (K)	Theoretical $q_m \times 10^{-5}$ (mol g ⁻¹)	Experimental $q \times 10^{-5}$ (mol g ⁻¹)	R ²	K_L (g/L)
298	4.12	3.52	0.996	0.2175
308	5.54	4.90	0.993	0.2592
318	5.87	5.30	0.99	0.2851

where q_e is the amount of the adsorbed dye at equilibrium, C_e is the dye concentration present in the solution at equilibrium, K_F is Freundlich isotherm constant related to the capacity of adsorption (mg/g or mol/g), n is empirical parameter signifies the intensity of adsorption and also shows the favourability of the process of adsorption, favorable ($0 < 1/n < 1$), irreversible ($1/n = 0$) and unfavorable ($1/n > 1$) [48]. If $n = 1$ then the partitions are concentration independent between the two phases. If $1/n$ value is below one it shows a normal sorption. On the other hand, $1/n$ value above one indicates the cooperative adsorption. Moreover, if n value lies between 1 and 10, then it shows that the adsorption process is favorable. The Freundlich isotherm in linearized form is given below:

$$\ln q_e = \ln K_F + 1/n \ln C_e \quad (7)$$

The value of $1/n$ and K_F can be obtained from the intercept and slope of the plot of $\log q_e$ versus C_e (Fig. 8). The values obtained for the coefficient of correlation (R^2) for Freundlich isotherm are found to be lesser than the Langmuir isotherm, suggesting that Langmuir isotherm is best fitted to experimental data. This model further assumes that the adsorbate concentration at the interface increases with its corresponding increase in the solution. If n value is equal to unity, then the adsorption process is linear. If n value is below unity, it shows the process of adsorption is unfavorable, and if the n value is above unity, then the process of adsorption is favorable. Further, if $1/n$ value is less than unity so it further confirms the normal Langmuir isotherm. As in our case, the value of $1/n$ is lesser than 1, so it confirms that the process of adsorption follows the Langmuir adsorption isotherm. If the value of n lies between 1 and 10 so it shows a beneficial process of adsorption. In the present work, the value of n for both dyes lies within this range. This implies that graphene oxide has a high affinity towards the rhodamine B and Congo red removal. The increase in the K_F value with increasing temperature indicates that the capacity of adsorption has been increased for the rhodamine B and Congo red adsorption onto the surface of graphene oxide. Further, the increase in the capacity of

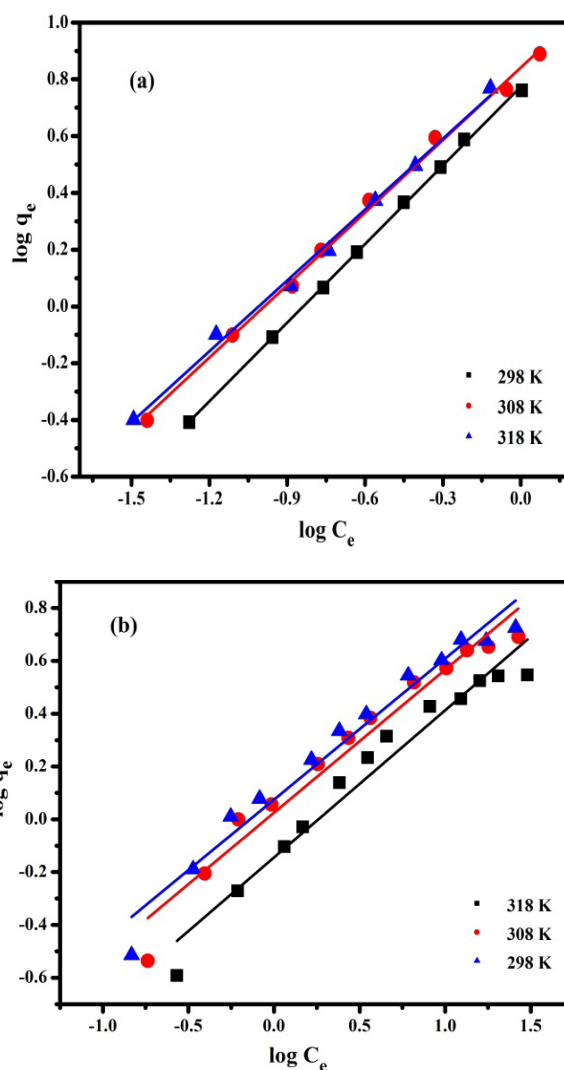


Fig. 8. Freundlich isotherm for the removal of dye (a) rhodamine B and (b) congo red onto the surface of graphene oxide at pH 7.

Freundlich adsorption with increasing temperature shows that the process of adsorption is endothermic in nature.

3.3.3. Dubinin–Radushkevich model for rhodamine B and Congo red adsorption

The Dubinin–Radushkevich (D-R) model can be used to estimate the adsorption free energy and characteristic porosity. It helps in the determination of the nature of the adsorption, i.e., whether the process is chemical or physical. The D–R isotherm is temperature dependent and it indicates the non-homogeneous surface of the adsorbent [48,49]. The D-R isotherm linear form is given below.

$$\ln q = \ln q_m - \beta \epsilon^2 \tag{8}$$

where q is the amount of adsorbed dye per unit weight of graphene oxide (mol/g), q_m is the maximum capacity of

adsorption (mol/g), while ϵ is the Polanyi potential and is equal to

$$\epsilon = RT \ln \left(1 + \frac{1}{C_e} \right) \tag{9}$$

where R is the general gas constant and its value is equal to 8.314 kJ/molK and T is the absolute temperature (K), β is the coefficient of activity associated with the adsorption mean free energy (mol²/kJ²), which is defined as “when one mole of ion from an infinity of solution is transferred to the solid surface then it is called free energy of adsorption and is represented by E ” as given by the following equation,

$$E = (2k)^{-0.5} \tag{10}$$

The process of physical adsorption occurs, when the $E < 8$ kJ/mol while $8 < E < 16$ shows that the chemical adsorption mechanism (ion-exchange). The Dubinin–Radushkevich model supported the mechanism of monolayer to be

Table 3
Freundlich parameters for the removal of rhodamine B onto the surface of graphene oxide at different temperatures and pH 7

Temperature(K)	1/n	K_F (L/g)	R^2
298	0.923	5.940	0.999
308	0.851	6.931	0.997
318	0.832	6.924	0.995

Table 4
Freundlich parameters for the removal of congo red onto the surface of graphene oxide at different temperatures and pH 7

Temperature (K)	1/n	K_F (L/g)	R^2
298	0.645	1.351	0.994
308	0.607	1.023	0.98
318	0.502	1.288	0.983

Table 5
D-R parameters for the removal of rhodamine B onto the surface of graphene oxide at different temperatures and pH 7

Temperature (K)	E (kJ mol ⁻¹)	R^2
298	2.307	0.97
308	2.570	0.98
318	2.470	0.91

Table 6
D-R parameters for the removal of congo red onto the surface of graphene oxide at different temperatures and pH 7

Temperature (K)	E (kJ mol ⁻¹)	R^2
298	0.516	0.94
308	0.594	0.91
318	0.527	0.92

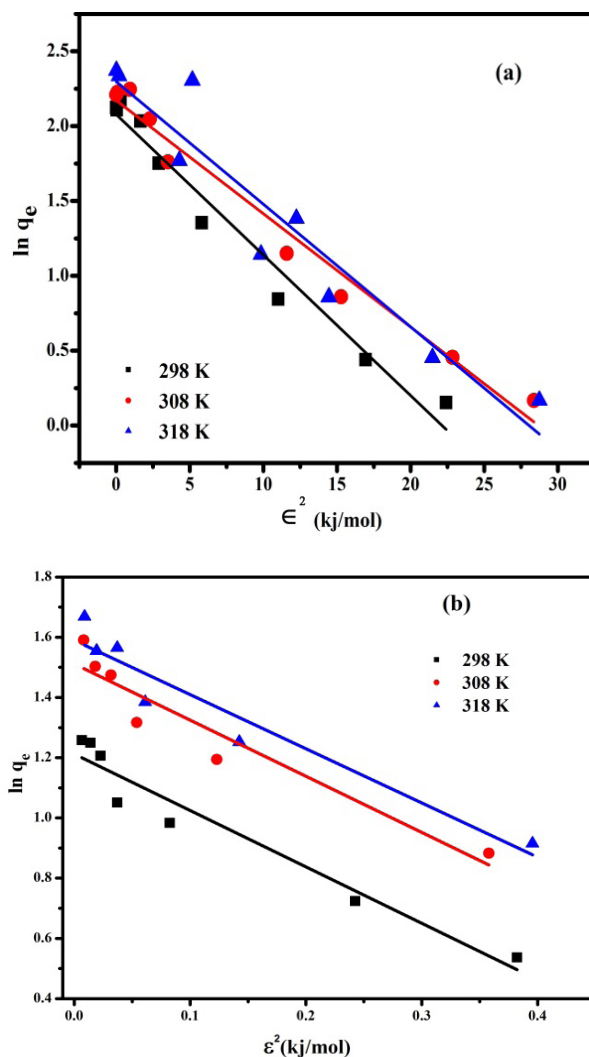


Fig. 9. D-R plots for the dye (a) rhodamine B and (b) congo red onto the surface of the graphene oxide at pH 7.

physical in nature because the mean free energy value was less than 8 kJ/mol.

3.4. Thermodynamic studies of rhodamine B and Congo red adsorption

The temperature effect on dyes adsorption is used to determine the important thermodynamic parameters such as Gibbs free energy, entropy and enthalpy change [18,50]. The influence of these parameters on the rhodamine B adsorption was calculated based on the following equations:

$$\Delta G = RT \ln K_c \quad (11)$$

$$\Delta G^\circ = \Delta H^\circ - T\Delta S^\circ \quad (12)$$

where ΔG is the Gibbs free energy change, R is the universal gas constant and its value is equal to 8.3145 J/molK, T is absolute temperature (K), and K_c is the constant of equilibrium and is given below:

$$K_c = \frac{C_e}{C_s} \quad (13)$$

where C_e is the equilibrium dye concentration and C_s is the dye concentration in solution. The standard enthalpy and entropy of the process of adsorption can be calculated by using the Van't Hoff equation:

$$\ln K_L = \frac{\Delta S^\circ}{R} - \frac{\Delta H^\circ}{RT} \quad (14)$$

The value of $\ln K_L$ was calculated from the Langmuir adsorption isotherm. The values of ΔH° and ΔS° were found to be 4.18 kJ·mol⁻¹ and 5.95 J·mol⁻¹ K⁻¹ respectively for rhodamine B, whereas, for Congo red the values of ΔH° and ΔS° were 10.69 kJ·mol⁻¹ and 8.80 J·mol⁻¹ K⁻¹ respectively. The ΔH° values of both dyes show that the removal was endothermic in nature. Moreover, the ΔS° values clearly indicates the irregular increase in the randomness at solid-liquid interface during the rhodamine B adsorption from aqueous solution onto the graphene oxide. The ΔS° value further indicates an increase in the degree of freedom of species adsorbed as reported elsewhere [18].

The Gibbs free energy (ΔG°) for the adsorption of rhodamine B and Congo red onto the graphene oxide was calculated by using Eq. (12). The negative value of ΔG° (Table 7) for rhodamine B and Congo red (Table 8) confirms that the removal process is spontaneous and thermodynamically favorable at all temperatures. As can be seen, that ΔG° value for rhodamine B changes from -1.77 to -1.89 kJ/mol whereas, the ΔG° value for Congo red changes from -2.61 to -2.78 kJ/mol. This indicates that the removal of rhodamine B and Congo red onto the surface of the graphene oxide at higher temperature is more spontaneous. Similar results were also reported by other researchers in the literature [51].

3.5. Adsorption mechanism

The mechanism of adsorption depends upon the texture properties and chemistry of the adsorbent and adsorbate.

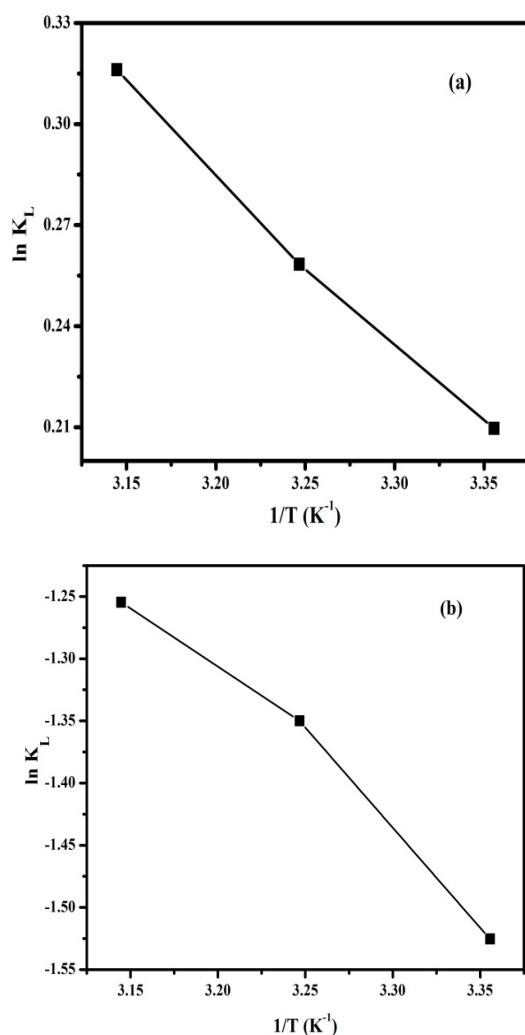


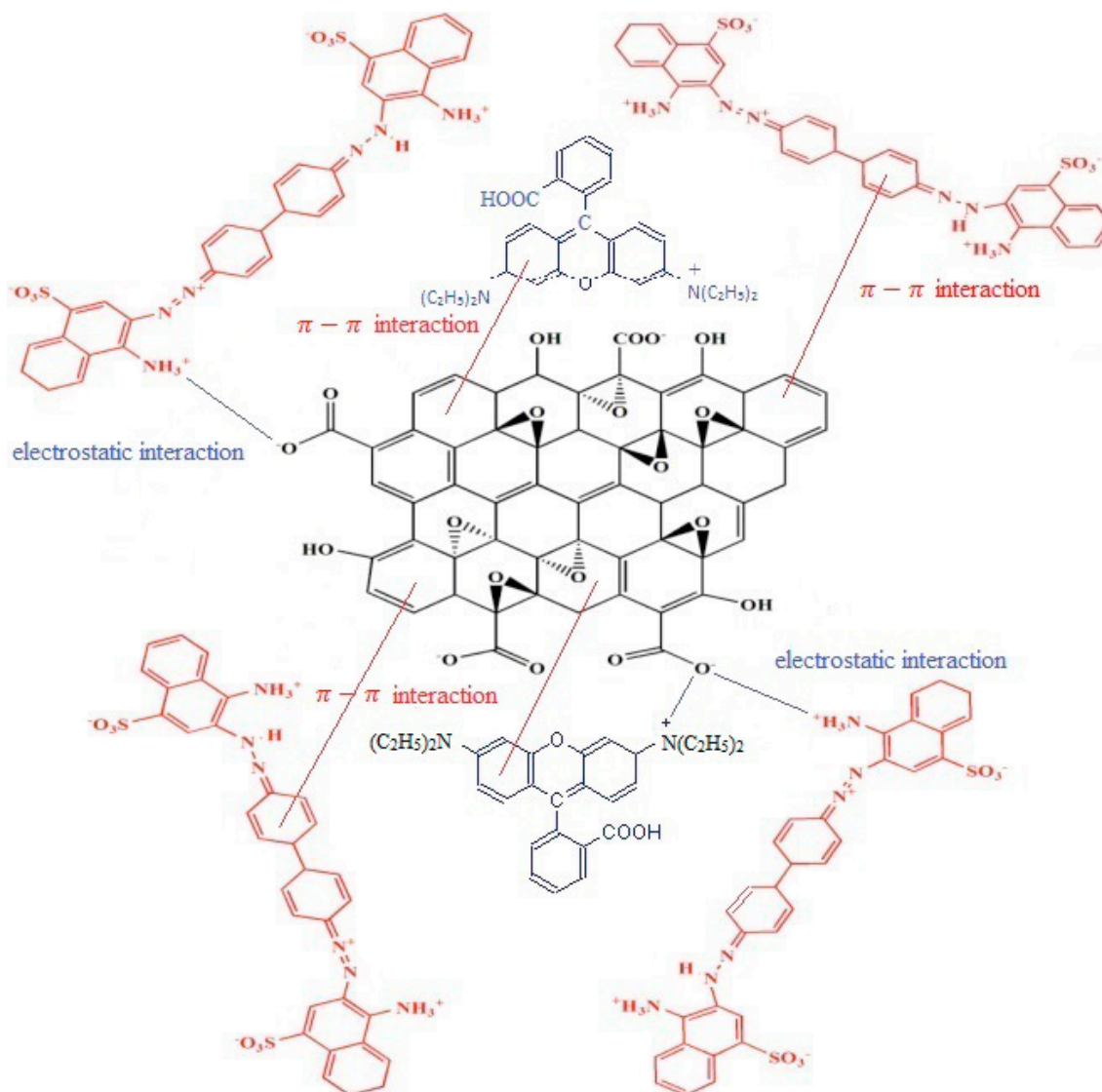
Fig. 10. Van't Hoff plot for the adsorption of dye (a) rhodamine B and (b) Congo red onto the surface of graphene oxide at pH 7.

Table 7
Thermodynamic parameters for the removal of rhodamine B onto the surface of graphene oxide

Temperature (K)	ΔG° (kJ mol ⁻¹)	ΔH° (kJ mol ⁻¹)	ΔS° (J mol ⁻¹ K ⁻¹)
298	-1.77	4.18	5.95
308	-1.83		
318	-1.89		

Table 8
Thermodynamic parameters for the removal of Congo red onto the surface of graphene oxide

Temperature (K)	ΔG° (kJ mol ⁻¹)	ΔH° (kJ mol ⁻¹)	ΔS° (J mol ⁻¹ K ⁻¹)
298	-2.61	10.69	8.80
308	-2.70		
318	-2.78		



Scheme 1. Mechanism of adsorption for the removal of rhodamine B and Congo red onto graphene oxide.

The forces that are involved in the process of adsorption are electrostatic attraction and interaction as shown in Scheme 1. The electrostatic attraction exists between the opposite charges on graphene oxide and both dyes rhodamine B and Congo red while the interactions occur between the aromatic ring of rhodamine B and Congo red and the aromatic ring of graphene oxide [52].

3.6. Comparison with other adsorbents

The adsorption capacity of graphene oxide for adsorption of rhodamine B and Congo red was compared with other adsorbents reported in the literature. The maximum adsorption capacity of graphene oxide was calculated to be 1655 mg/g, which is higher than the adsorption capacities of other adsorbents as shown in Table 9. Postai et al. [53] investigated the removal of rhodamine B from waste water by using the waste seeds *Aleurites moluccana* (WAM) as an adsorbent. The maximum adsorption capacity of

rhodamine B was 117 mg/g. Peng et al. [54] used the humic acid modified Fe_3O_4 nanoparticles ($\text{Fe}_3\text{O}_4/\text{HA}$) for the adsorption of rhodamine B from aqueous solution and the maximum adsorption capacity was reported to be 161.8 mg/g. Khan et al. [55] reported the kaolinite adsorption efficiency for the removal of rhodamine B from aqueous solution and the maximum adsorption capacity for rhodamine B adsorption was 46.08 mg/g. Zhou et al. [56] used the shrimp shell powder for the removal of Congo red from waste water. Results revealed that adsorption capacity for treated shrimp shell powder was 288.2 mg/g for the removal of Congo red. The above study suggest that graphene oxide may be used as an excellent adsorbent for the removal of rhodamine B and Congo red from aqueous solution due to the presence of different oxygen functional groups, high surface area and high adsorption capacity. Therefore, graphene oxide has a great potential to be applied for the treatment of waste water in the near future.

Table 9
Comparison of adsorption capacities of rhodamine B and congo red by graphene oxide with other adsorbents

Adsorbent	q_{max} (mg/g)	References
Waste seeds <i>Aleurites moluccana</i> (WAM)	117	[53]
Humic acid (HA) modified Fe_3O_4 nanoparticles	161.8	[54]
Kaolinite	46.08	[55]
Shrimp shell powder	288.2	[56]
Duolite C-20 (resin)	28.57	[57]
Activated Carbon	6.72	[58]
Montmorillonite	8.4	[59]
Graphene Oxide	1655	This Study

4. Conclusion

Graphene oxide was successfully synthesized by modified Hummer's method. The various analytical techniques such as thermogravimetric/differential thermal analysis, scanning electron microscopy, fourier transform infrared spectrometry and X-ray diffraction were used to evaluate the physiochemical properties of the synthesized graphene oxide. The synthesized graphene oxide showed potential capacity towards adsorption of rhodamine B and Congo red. However, it was found that graphene oxide showed greater affinity towards the adsorption of rhodamine B as compared to Congo red. This may be due to the strong electrostatic interaction between the positively charged surface of rhodamine B and negatively charged surface of graphene oxide. Moreover, the thermodynamic parameters such as ΔH° , ΔS° and ΔG° calculated in this study, clearly indicated that the adsorption process of the selected dyes on graphene oxide was physisorption, endothermic and spontaneous at all temperatures. Thus, graphene oxide may be used as a potential adsorbent for the removal of toxic pollutants from drinking water.

References

- [1] S. Khan, A.M. Khan, M.N. Khan, Investigation of pollutants load in waste water of Hayatabad Industrial Estate, Peshawar, Pakistan, Pak. J. Appl. Sci., 2 (2002) 457–461.
- [2] A. Azizullah, M.N.K. Khattak, P. Richter, D.-P. Häder, Water pollution in Pakistan and its impact on public health—a review, Environ. Int., 37 (2011) 479–497.
- [3] H. Chaudhuri, S. Dash, A. Sarkar, SBA-15 functionalised with high loading of amino or carboxylate groups as selective adsorbent for enhanced removal of toxic dyes from aqueous solution, New. J. Chem., 40 (2016) 3622–3634.
- [4] D. Şolpan, S. Duran, D. Saraydin, O. Güven, Adsorption of methyl violet in aqueous solutions by poly (acrylamide-co-acrylic acid) hydrogels, Radiat. Phys. Chem., 66 (2003) 117–127.
- [5] W.C. Wanyonyi, J.M. Onyari, P.M. Shiundu, Adsorption of Congo Red Dye from aqueous solutions using roots of Eichhornia crassipes: kinetic and equilibrium studies, Energy Procedia, 50 (2014) 862–869.
- [6] M.N. Ashiq, M. Najam-UL-Haq, T. Amanat, A. Saba, A.M. Qureshi, M. Nadeem, Removal of methylene blue from aqueous solution using acid/base treated rice husk as an adsorbent, Desal. Water Treat., 49 (2012) 376–383.
- [7] S. Guiza, M. Bagane, Adsorption of dyes from aqueous solution under batch mode using cellulosic orange peel waste, Desal. Water Treat., 113 (2018) 262–269.
- [8] M.A.M. Salleh, D.K. Mahmoud, W.A.W.A. Karim, A. Idris, Cationic and anionic dye adsorption by agricultural solid wastes: A comprehensive review, Desalination, 280 (2011) 1–13.
- [9] V. Gupta, Application of low-cost adsorbents for dye removal—A review, J. Environ. Manage., 90 (2009) 2313–2342.
- [10] Y.L. Pang, A.Z. Abdullah, Current status of textile industry wastewater management and research progress in Malaysia: a review, Clean-Soil, Air, Water, 41 (2013) 751–764.
- [11] M.K. Purkait, A. Maiti, S. Dasgupta, S. De, Removal of Congo red using activated carbon and its regeneration, J. Hazard. Mater., 145 (2007) 287–295.
- [12] H. Chaudhuri, S. Dash, A. Sarkar, Fabrication of new synthetic routes for functionalized Si-MCM-41 materials as effective adsorbents for water remediation, Ind. Eng. Chem. Res., 55 (2016) 10084–10094.
- [13] V. Vimonses, S. Lei, B. Jin, C.W. Chow, C. Saint, Adsorption of Congo red by three Australian kaolins, Appl. Clay Sci., 43 (2009) 465–472.
- [14] B. Cuiping, X. Xianfeng, G. Wenqi, F. Dexin, X. Mo, G. Zhongxue, X. Nian, Removal of rhodamine B by ozone-based advanced oxidation process, Desalination, 278 (2011) 84–90.
- [15] M. Aliabadi, T. Sagharigar, Photocatalytic removal of Rhodamine B from aqueous solutions using TiO_2 nanocatalyst, J. Appl. Environ. Biol. Sci., 1 (2011) 620–626.
- [16] G. Muthuraman, T.T. Teng, Extraction and recovery of rhodamine B, methyl violet and methylene blue from industrial wastewater using D_2EHPA as an extractant, J. Ind. Eng. Chem., 15 (2009) 841–846.
- [17] P. Bartasus, H. Cieśliński, A. Bujacz, A. Wierzbicka-Woś, J. Kur, A study on the interaction of rhodamine B with methylthioadenosine phosphorylase protein sourced from an Antarctic soil metagenomic library, PLoS One, 8 (2013) e55697.
- [18] M. Mohammadi, A.J. Hassani, A.R. Mohamed, G.D. Najafpour, Removal of rhodamine B from aqueous solution using palm shell-based activated carbon: adsorption and kinetic studies, J. Chem. Eng. Data, 55 (2010) 5777–5785.
- [19] H. Chaudhuri, S. Dash, A. Sarkar, Single-step room-temperature in situ syntheses of sulfonic acid functionalized SBA-16 with ordered large pores: potential applications in dye adsorption and heterogeneous catalysis, Ind. Eng. Chem. Res., 56 (2017) 2943–2957.
- [20] M. Doğan, M. Alkan, Removal of methyl violet from aqueous solution by perlite, J. Colloid Interface Sci., 267 (2003) 32–41.
- [21] L. Ai, M. Li, L. Li, Adsorption of methylene blue from aqueous solution with activated carbon/cobalt ferrite/alginate composite beads: kinetics, isotherms, and thermodynamics, J. Chem. Eng. Data, 56 (2011) 3475–3483.
- [22] M. Doğan, Y. Özdemir, M. Alkan, Adsorption kinetics and mechanism of cationic methyl violet and methylene blue dyes onto sepiolite, Dyes Pigm., 75 (2007) 701–713.
- [23] M.M. Ayad, A.A. El-Nasr, Adsorption of cationic dye (methylene blue) from water using polyaniline nanotubes base, J. Phys. Chem. C, 114 (2010) 14377–14383.
- [24] D. Lakherwal, Adsorption of heavy metals: a review, Int. J. Environ. Res. Dev., 4 (2014) 41–48.
- [25] A. Mittal, J. Mittal, A. Malviya, V. Gupta, Adsorptive removal of hazardous anionic dye “Congo red” from wastewater using waste materials and recovery by desorption, J. Colloid Interface Sci., 340 (2009) 16–26.
- [26] J. Chen, B. Yao, C. Li, G. Shi, An improved Hummers method for eco-friendly synthesis of graphene oxide, Carbon, 64 (2013) 225–229.
- [27] G. Venugopal, K. Krishnamoorthy, R. Mohan, S.-J. Kim, An investigation of the electrical transport properties of graphene-oxide thin films, Mater. Chem. Phys., 132 (2012) 29–33.
- [28] K. Krishnamoorthy, M. Veerapandian, K. Yun, S.-J. Kim, The chemical and structural analysis of graphene oxide with different degrees of oxidation, Carbon, 53 (2013) 38–49.

- [29] G. Titelman, V. Gelman, S. Bron, R. Khalfin, Y. Cohen, H. Bianco-Peled, Characteristics and microstructure of aqueous colloidal dispersions of graphite oxide, *Carbon*, 43 (2005) 641–649.
- [30] C. Xu, X. Wang, J. Zhu, X. Yang, L. Lu, Deposition of Co_3O_4 nanoparticles onto exfoliated graphite oxide sheets, *J. Mater. Chem.*, 18 (2008) 5625–5629.
- [31] S. Chaiyakun, N. Witit-Anun, N. Nuntawong, P. Chindaudom, S. Oaew, C. Kedkeaw, P. Limsuwan, Preparation and characterization of graphene oxide nanosheets, *Procedia Eng.*, 32 (2012) 759–764.
- [32] P. Bhawal, S. Ganguly, T. Chaki, N. Das, Synthesis and characterization of graphene oxide filled ethylene methyl acrylate hybrid nanocomposites, *RSC Adv.*, 6 (2016) 20781–20790.
- [33] R. Zhang, M. Hummelgård, G. Lv, H. Olin, Real time monitoring of the drug release of rhodamine B on graphene oxide, *Carbon*, 49 (2011) 1126–1132.
- [34] C. Lei, M. Pi, C. Jiang, B. Cheng, J. Yu, Synthesis of hierarchical porous zinc oxide (ZnO) microspheres with highly efficient adsorption of Congo red, *J. Colloid Interface Sci.*, 490 (2017) 242–251.
- [35] J. Zhao, Z. Wang, J.C. White, B. Xing, Graphene in the aquatic environment: adsorption, dispersion, toxicity and transformation, *Environ. Sci. Technol.*, 48 (2014) 9995–10009.
- [36] I. Chowdhury, M.C. Duch, N.D. Mansukhani, M.C. Hersam, D. Bouchard, Colloidal properties and stability of graphene oxide nanomaterials in the aquatic environment, *Environ. Sci. Technol.*, 47 (2013) 6288–6296.
- [37] P. Sharma, M.R. Das, Removal of a cationic dye from aqueous solution using graphene oxide nanosheets: investigation of adsorption parameters, *J. Chem. Eng. Data*, 58 (2012) 151–158.
- [38] G. Crini, H.N. Peindy, F. Gimbert, C. Robert, Removal of CI Basic Green 4 (Malachite Green) from aqueous solutions by adsorption using cyclodextrin-based adsorbent: Kinetic and equilibrium studies, *Sep. Purif. Technol.*, 53 (2007) 97–110.
- [39] R. Ahmad, R. Kumar, Adsorptive removal of Congo red dye from aqueous solution using bael shell carbon, *Appl. Surf. Sci.*, 257 (2010) 1628–1633.
- [40] R. Zhang, J. Zhang, X. Zhang, C. Dou, R. Han, Adsorption of Congo red from aqueous solutions using cationic surfactant modified wheat straw in batch mode: kinetic and equilibrium study, *J. Taiwan Inst. Chem. Eng.*, 45 (2014) 2578–2583.
- [41] M. Said, R.L. Machunda, Defluoridation of water supplies using coconut shells activated carbon: batch studies, *Int. J. Sci. Res. (IJSR)*, 3 (2014) 2327–2331.
- [42] S. Cheng, L. Zhang, A. Ma, H. Xia, J. Peng, C. Li, J. Shu, Comparison of activated carbon and iron/cerium modified activated carbon to remove methylene blue from wastewater, *J. Environ. Sci.*, 65 (2018) 92–102.
- [43] I. Langmuir, The constitution and fundamental properties of solids and liquids. Part I. Solids, *J. Am. Chem. Soc.*, 38 (1916) 2221–2295.
- [44] S. Cheng, L. Zhang, H. Xia, J. Peng, J. Shu, C. Li, Ultrasound and microwave-assisted preparation of Fe-activated carbon as an effective low-cost adsorbent for dyes wastewater treatment, *RSC Adv.*, 6 (2016) 78936–78946.
- [45] S.M. Al-Rashed, A.A. Al-Gaid, Kinetic and thermodynamic studies on the adsorption behavior of Rhodamine B dye on Duolite C-20 resin, *J. Saudi Chem. Soc.*, 16 (2012) 209–215.
- [46] S. Cheng, Q. Chen, H. Xia, L. Zhang, J. Peng, G. Lin, X. Liao, X. Jiang, Q. Zhang, Microwave one-pot production of $\text{ZnO}/\text{Fe}_3\text{O}_4$ /activated carbon composite for organic dye removal and the pyrolysis exhaust recycle, *J. Cleaner Prod.*, 188 (2018) 900–910.
- [47] H. Freundlich, Over the adsorption in solution, *J. Phys. Chem.*, 57 (1906) 1100–1107.
- [48] M.R.R. Kooh, M.K. Dahri, L.B. Lim, The removal of rhodamine B dye from aqueous solution using Casuarina equisetifolia needles as adsorbent, *Cogent Environ. Sci.*, 2 (2016) 1140553.
- [49] S. Cheng, L. Zhang, H. Xia, J. Peng, J. Shu, C. Li, X. Jiang, Q. Zhang, Adsorption behavior of methylene blue onto waste-derived adsorbent and exhaust gases recycling, *RSC Adv.*, 7 (2017) 27331–27341.
- [50] H. Chaudhuri, S. Dash, R. Gupta, D.D. Pathak, A. Sarkar, Room-temperature in-situ design and use of graphene Oxide-SBA-16 composite for water remediation and reusable heterogeneous catalysis, *Chemistry select*, 2 (2017) 1835–1842.
- [51] M. Ghaedi, J. Tashkhourian, A.A. Pebdani, B. Sadeghian, F.N. Ana, Equilibrium, kinetic and thermodynamic study of removal of reactive orange 12 on platinum nanoparticle loaded on activated carbon as novel adsorbent, *Korean J. Chem. Eng.*, 28 (2011) 2255–2261.
- [52] H.N. Tran, Y.-F. Wang, S.-J. You, H.-P. Chao, Insights into the mechanism of cationic dye adsorption on activated charcoal: the importance of π - π interactions, *Process Saf. Environ. Prot.*, 107 (2017) 168–180.
- [53] D.L. Postai, C.A. Demarchi, F. Zanatta, D.C.C. Melo, C.A. Rodrigues, Adsorption of rhodamine B and methylene blue dyes using waste of seeds of Aleurites Moluccana, a low cost adsorbent, *Alexandria Eng. J.*, 55 (2016) 1713–1723.
- [54] L. Peng, P. Qin, M. Lei, Q. Zeng, H. Song, J. Yang, J. Shao, B. Liao, J. Gu, Modifying Fe_3O_4 nanoparticles with humic acid for removal of Rhodamine B in water, *J. Hazard. Mater.*, 209 (2012) 193–198.
- [55] T.A. Khan, S. Dahiya, I. Ali, Use of kaolinite as adsorbent: Equilibrium, dynamics and thermodynamic studies on the adsorption of Rhodamine B from aqueous solution, *Appl. Clay Sci.*, 69 (2012) 58–66.
- [56] Y. Zhou, L. Ge, N. Fan, M. Xia, Adsorption of Congo red from aqueous solution onto shrimp shell powder, *Adsorpt. Sci. Technol.*, 36 (2018) 1310–1330.
- [57] S.M. Al-Rashed, A.A. Al-Gaid, Kinetic and thermodynamic studies on the adsorption behavior of Rhodamine B dye on Duolite C-20 resin, *J. Saudi Chem. Soc.*, 16 (2012) 209–215.
- [58] C. Namasivayam, D. Kavitha, Removal of Congo Red from water by adsorption onto activated carbon prepared from coir pith, an agricultural solid waste, *Dyes Pigm.*, 54 (2002) 47–58.
- [59] Y.O. Khaniabadi, H. Basiri, H. Nourmoradi, M.J. Mohammadi, A.R. Yari, S. Sadeghi, A. Amrane, Adsorption of Congo Red Dye from aqueous solutions by montmorillonite as a low-cost adsorbent, *Int. J. Chem. React. Eng.*, 16 (2018).